Comput Mech (2005) 35: 342–351
DOI 10.1007/s00466-004-0621-x

ORIGINAL PAPER

Suh-Jenq Yang · Teng-Ruey Chang · Wu-Shung Fu

Numerical simulation of flow structures around an oscillating rectangular cylinder in a channel flow

Received: 19 March 2003 / Accepted: 13 August 2004 / Published online: 22 September 2004

Abstract In this paper, the flow structures of a confined flow over a transversely oscillating rectangular cylinder are investigated numerically. The flow characteristics are dynamic and are classified as a moving boundary problem. An arbitrary Lagrangian-Eulerian (ALE) kinematic description method is used to describe the flow field and a Galerkin finite element formulation with moving meshes is employed to solve the governing equations. The effects of the oscillating speed, frequency and aspect ratio on the flow field are examined. The initiation and subsequent developments of the vortex shedding are investigated in details. The results indicate that the vortices shedding from the rectangular cylinder are entrained by the motion of the rectangular cylinder, and the interactions between the oscillating rectangular cylinder and shedding vortices dominate the state of the wake. The vortex shedding frequency is gradually changed to match the rectangular cylinder oscillating frequency, and the flow field may approach a periodic motion with time. The mechanisms of the vortex shedding from an oscillating rectangular cylinder are different from those of an oscillating circular cylinder.

List of symbols

A	aspect ratio ($A = w_2/h_2$)
A_c	dimensionless oscillating amplitude of the rectangular cylinder
f	dimensional vortex shedding frequency (s^{-1})
h	dimensional height of the channel (m)
H	dimensionless height of the channel ($H = h/h_2$)
n	normal vector of coordinates
n_e	number of elements
p	dimensional pressure ($N \cdot m^{-2}$)
p_∞	referential pressure ($N \cdot m^{-2}$)
P	dimensionless pressure ($P = (p - p_\infty)/\rho u_0^2$)
Re	Reynolds number ($Re = u_0 h_2/v$)
St	Strouhal number ($St = f h_2/u_0$)
t	dimensional time (s)
u, v	dimensional velocities in x and y directions ($m \cdot s^{-1}$)
U, V	dimensionless velocities in X and Y directions ($U = u/u_0$, $V = v/u_0$)
u_0	dimensional velocity of the inlet fluid ($m \cdot s^{-1}$)
$\hat{u}$, $\hat{v}$	dimensional mesh velocity in x and y directions ($m \cdot s^{-1}$)
$\hat{U}$, $\hat{V}$	dimensionless mesh velocity in X and Y directions ($\hat{U} = \hat{u}/u_0$, $\hat{V} = \hat{v}/u_0$)
v_c	dimensional oscillating velocity of the rectangular cylinder ($m \cdot s^{-1}$)
V_c	dimensionless oscillating velocity of the rectangular cylinder ($V_c = v_c/u_0$)
v_m	dimensional maximum oscillating speed of the rectangular cylinder ($m \cdot s^{-1}$)
V_m	dimensionless maximum oscillating speed of the rectangular cylinder ($V_m = v_m/u_0$)
w	dimensional length of the channel (m)
W	dimensionless length of the channel ($W = w/h_2$)
w_2	dimensional width of the rectangular cylinder (m)
W_2	dimensionless width of the rectangular cylinder ($W_2 = w_2/h_2$)
x, y	dimensional Cartesian coordinates (m)
X, Y	dimensionless Cartesian coordinates ($X = x/h_2$, $Y = y/h_2$)

Greek symbols

λ	penalty parameter
v	kinematic viscosity ($m^2 \cdot s^{-1}$)
ρ	density ($kg \cdot m^{-3}$)
τ	dimensionless time ($\tau = tu_0/h_2$)
τ_p	dimensionless time of one cycle

S.-J. Yang (✉) · T.-R. Chang
Department of Industrial Engineering and Management,
Nan Kai College, Nantou 54210, Taiwan
E-mail: sjyang@nkc.edu.tw
Fax: 886-49-2565842

W.-S. Fu
Department of Mechanical Engineering,
National Chiao-Tung University, Hsinchu 30010, Taiwan

ω dimensional oscillating frequency of the rectangular cylinder (s^{-1})
Ω dimensionless oscillating frequency of the rectangular cylinder ($\Omega = \omega h_2/u_0$)
Ψ dimensionless stream function

Superscripts

(e) element
m iteration number
T transpose matrix

Other

[ ] matrix
{ } column vector
⟨ ⟩ row vector
| | absolute value

1 Introduction

Investigations of characteristics of a flow passing structures are mainly focused on the vortex shedding and flow-induced vibration, which can alter the frequency and intensity of the forces acting on structures. These characteristics are very important to engineering applications.

Several numerical and experimental studies had been done to study an unsteady flow induced by a stationary circular cylinder or an oscillating circular cylinder [1–8]. The attentions of these studies were focused on the mechanisms of vortex shedding, vortex shedding frequency or Strouhal number, and lock-in state. The results showed that Strouhal number was about 0.2 over a range of the Reynolds number varying from 2×10^2 to 10^4 for a stationary circular cylinder.

Instead of the circular cylinder mentioned above, rectangular cylinder also is a typical structure used in engineering applications. Some numerical and experimental studies have been conducted on this subject to investigate the variations of the flow structures [9–15]. These studies primarily concerned with the unsteady characteristics of the vortex shedding frequency or Strouhal number of the flow structures as the fluid flows over a stationary rectangular cylinder. The results demonstrated that the blockage ratio, aspect ratio and attack angle of the rectangular cylinder were the major effective factors of the flow characteristics.

Must studies mentioned above focused on a stationary rectangular cylinder or an oscillating flow. However, to the knowledge of the author, the vortex shedding flow from an oscillating rectangular cylinder in a flow is seldom investigated. This could be applied in moving machine, eddy promoter, flow-control problems, and so on. Therefore, the purpose of the present study is to investigate numerically the variations of flow structures induced by a transversely oscillating rectangular cylinder in a channel flow.

Because of the interaction between the flow and oscillating rectangular cylinder, the variations of the flow field become time-dependent state and are classified as a type of moving boundary problems. In the past, a structure oscillating or moving in a flow was conveniently analyzed using a non-inertial reference frame, which is moving with the structure. However, as the structure oscillates or moves in the flow, the structure will press the fluid near the structure, and the fluid near the structure will simultaneously replenish the vacant space induced by the movement of the structure. The non-inertial reference frame could not describe these flows realistically.

For simulating the problem mentioned above more realistically, the moving interfaces between the fluid and oscillating structure have to be considered. Thus, either the Lagrangian or Eulerian method is hardly utilized to analyze this problem solely. An arbitrary Lagrangian–Eulerian (ALE) kinematic description method [16], which combines the characteristics of the Lagrangian and Eulerian methods, is an appropriate method to describe this problem. In the ALE method, the computational meshes may move with the fluid (Lagrangian), be held fixed (Eulerian), or be moved in a prescribed way. The detail of the kinematic theory of the ALE method is delineated in Hughes et al. [17], Donea et al. [18], Kawahara and Ramaswamy [19], and Ramaswamy [20].

Consequently, in this paper, the ALE kinematic description method is utilized to analyze numerically the flow structures induced by an oscillating rectangular cylinder. A Galerkin finite element method and a backward difference scheme, dealing with the time differential terms, are applied to solve the governing equations. The initiation and subsequent developments of the vortex shedding are investigated in detail. The variations in the oscillating speed, frequency and aspect ratio are considered.

2 Physical model

The physical model is showed in Fig. 1. A two-dimensional channel with height h and length w is used to simulate this problem. A rectangular cylinder with width w_2 and height h_2 is set within this channel. The distance

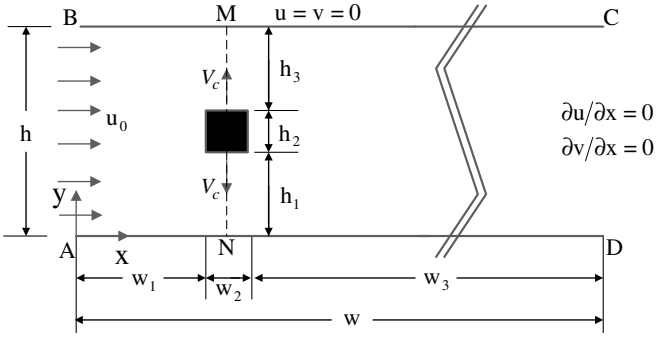

Fig. 1 Physical model

from the inlet of the channel to the rectangular cylinder is w_1. The inlet velocity u_0 of the fluid is uniform. Initially ($t = 0$), the rectangular cylinder is stationary at the position of the center of the channel and the fluid flows steadily. The distance from the wall of the channel to the rectangular cylinder is h_1. As the time $t > 0$, the rectangular cylinder is forced to oscillate in the transverse direction. The behavior of the oscillating rectangular cylinder and flow is then coupled, and the variations of the flow field become time-dependent state and are classified as a moving boundary problem. Thus, it is best to use the ALE method to analyze this problem.

For analyzing conveniently, the rectangular cylinder is assumed to oscillate with a velocity $v_m \cos(2\pi\omega t)$in the transverse direction, where ω and v_c are the oscillating frequency and maximum oscillating speed of the rectangular cylinder, respectively. Furthermore, the following assumptions are made.

(1) The flow field is two-dimensional, incompressible and laminar.
(2) The fluid properties are constant and the effect of the gravity is neglected.
(3) The no-slip condition is held on the interfaces between the fluid and rectangular cylinder.

Based upon the characteristic scales of h_2, u_0, and ρu_0^2, the dimensionless variables are defined as follows:

$$X = \frac{x}{h_2}, \quad \mathrm{Y} = \frac{\mathrm{y}}{h_2}, \quad \mathrm{U} = \frac{\mathrm{u}}{u_0}, \quad \mathrm{V} = \frac{\mathrm{v}}{u_0},$$

$$\hat{U} = \frac{\hat{u}}{u_0}, \quad \hat{V} = \frac{\hat{v}}{u_0}, \quad V_{\mathrm{m}} = \frac{v_m}{u_0}, \quad \Omega = \frac{\omega \mathrm{h}_2}{u_0}, \tag{1}$$

$$P = \frac{p - p_\infty}{\rho u_0^2}, \quad \tau = \frac{t u_0}{h_2} \quad \mathrm{Re} = \frac{u_0 h_2}{v},$$

where $\hat{u}$ and $\hat{v}$ are the mesh velocities in the x and y directions, respectively.

According to the above assumptions and dimensionless variables, the dimensionless ALE governing equations are expressed as the following equations:

continuity equation

$$\frac{\partial U}{\partial X} + \frac{\partial V}{\partial Y} = 0, \tag{2}$$

momentum equations

$$\frac{\partial U}{\partial \tau} + (U - \hat{U})\frac{\partial U}{\partial X} + (V - \hat{V})\frac{\partial U}{\partial Y} = -\frac{\partial P}{\partial X} + \frac{1}{\mathrm{Re}}\left(\frac{\partial^2 U}{\partial X^2} + \frac{\partial^2 U}{\partial Y^2}\right), \tag{3}$$

$$\frac{\partial V}{\partial \tau} + (U - \hat{U})\frac{\partial V}{\partial X} + (V - \hat{V})\frac{\partial V}{\partial Y} = -\frac{\partial P}{\partial Y} + \frac{1}{\mathrm{Re}}\left(\frac{\partial^2 V}{\partial X^2} + \frac{\partial^2 V}{\partial Y^2}\right). \tag{4}$$

As the time $\tau > 0$, the boundary conditions are as follows:

on the fluid inlet surface AB

$$U = 1, \quad V = 0, \tag{5}$$

on the walls of the channel BC and AD

$$U = \mathrm{V} = 0, \tag{6}$$

on the fluid outlet surface CD

$$\partial U/\partial n = \partial V/\partial n = 0, \tag{7}$$

on the interfaces between the fluid and rectangular cylinder

$$U = 0, \quad \mathrm{V} = \mathrm{V_m}\cos(2\pi\Omega\tau). \tag{8}$$

3 Numerical method

The governing equations and boundary conditions are solved through the Galerkin finite element formulation with moving meshes. A backward scheme is adopted to deal with the time differential terms of the governing equations. The pressure is eliminated from the governing equations using the penalty function method [21]. The velocity terms are approximated by quadrilateral elements and nine-node quadratic Lagrangian interpolation function, and the shape function is utilized as the weighting function. The Newton-Raphson iteration algorithm is utilized to simplify the nonlinear terms in the momentum equations. The discretization processes of the governing equations are similar to the one used in Hueber et al. [22]. Then, the momentum equations (3) and (4) can be expressed as the following matrix form:

$$\sum_{1}^{n_e}\left([A]^{(e)} + [K]^{(e)} + \lambda[L]^{(e)}\right)\{q\}^{(e)}_{\tau+\Delta\tau} = \sum_{1}^{n_e}\{f\}^{(e)}, \tag{9}$$

where

$$(\{q\}^{(e)}_{\tau+\Delta\tau})^T = \langle U_1, \mathrm{U}_2, \ldots, \mathrm{U}_9, \mathrm{V}_1, \mathrm{V}_2, \ldots, \mathrm{V}_9\rangle^{m+1}_{\tau+\Delta\tau}, \tag{10}$$

$[A]^{(e)}$ includes the (m)th iteration values of U and V at time $\tau + \Delta\tau$,
$[K]^{(e)}$ includes the shape function, mesh velocity, and time differential terms,
$[L]^{(e)}$ includes the penalty function terms,
$\{f\}^{(e)}$ includes the known values of U and V at time τ and (m)th iteration values of U and V at time $\tau + \Delta\tau$.

In Eq. (9), a Gaussian quadrature procedure is conveniently used to execute the numerical integration. The terms with the penalty parameter λ are integrated by a 2×2 Gaussian quadrature, and the other terms are integrated by a 3×3 Gaussian quadrature [21, 22]. The value of penalty parameter λ used in this study is 10^6. The frontal method solver [23, 24] is applied to solve equation (9).

Because of the rectangular cylinder oscillating in the transverse direction only, the mesh velocity in the X direction is assigned to be zero, i.e., $\hat{U} = 0$. As for the mesh velocity in the Y direction, $\hat{V}$, it is assumed to be linearly distributed and inversely proportional to the distance between the nodes of the computational elements and the rectangular cylinder.

A brief outline of the solution procedures are described as follows:

(1) Determine the optimal mesh distribution and number of the elements and nodes.
(2) Solve the values of the U and V at the steady state ($\tau = 0.0$) and regard them as the initial values.
(3) Determine the time step $\Delta\tau$ and the mesh velocities.
(4) Update the coordinates of the nodes and examine the determinant of the Jacobian transformation matrix to ensure that the one-to-one mapping is satisfied during the Gaussian quadrature numerical integration.
(5) Solve equation (9), until the following criteria for convergence are satisfied:

$$\left|\frac{\phi^{m+1} - \phi^{m}}{\phi^{m+1}}\right|_{\tau+\Delta\tau} < 10^{-3}, \text{ where } \phi = \mathrm{U}, \mathrm{V} \qquad (11)$$

(6) Continue the next time step calculation until periodic solutions are obtained.

The numerical scheme and code are developed by the author and have been validated in the previous studies [25, 26].

4 Results and discussion

For satisfying the boundary conditions at the inlet and outlet of the channel mentioned earlier, the lengths from the inlet and outlet to the rectangular cylinder are determined by numerical tests and equal to 8.0 and 21.0, respectively. At the time $\tau = 0$, the rectangular cylinder is at the position of the center of the channel. The effects of the oscillating frequency Ω, maximum oscillating speed V_m and aspect ratio A of the rectangular cylinder on the flow characteristics under Re = 500 are studied in details. Table 1 shows the parameter combination for each case. In addition, the dimensionless vortex shedding frequency, i.e., Strouhal number St, is defined as $St = fh_2/u_0$, where f is the vortex shedding frequency.

Table 1 Computed Parameter combinations

	V_m	τ_p	Ω	A_c	A
case 1	0.333	6.0	0.167	$1/\pi$	1.0
case 2	0.5	4.0	0.25	$1/\pi$	1.0
case 3	1.0	2.0	0.5	$1/\pi$	1.0
case 4	0.333	6.0	0.167	$1/\pi$	2.0

4.1 Mesh tests

Initially, a mesh-independence study is conducted to choose the proper computational meshes for the following numerical calculations. Three different nonuniform distributed elements, which provide fine elements near the rectangular cylinder and walls and sparse elements in the far field, are carried out for the mesh tests. The results of the velocities U and V distributions along the line $\overline{MN}$ as indicated in Fig. 1 at the steady state under Re = 500 and $A = 1.0$ situation are shown in Fig. 2. Based upon

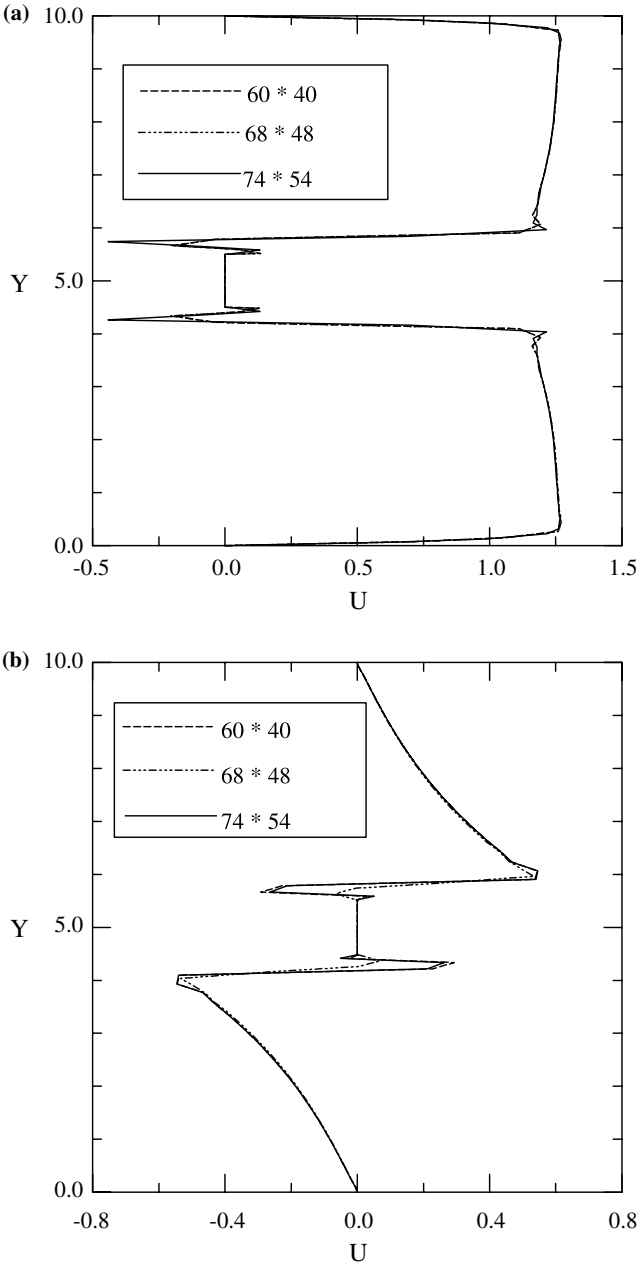

Fig. 2 Comparison of the velocity profiles along the line $\overline{MN}$ at the steady state of Re = 500 , and $A = 1.0$ situation for various computational elements

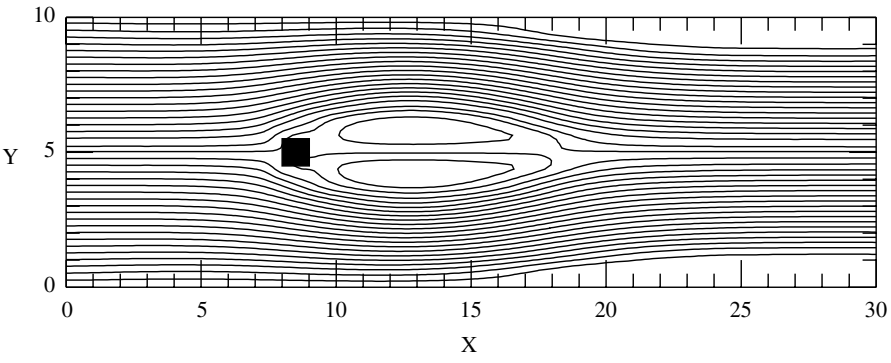

Fig. 3 The distribution of streamlines at the steady state of Re = 500 and $A = 1.0$

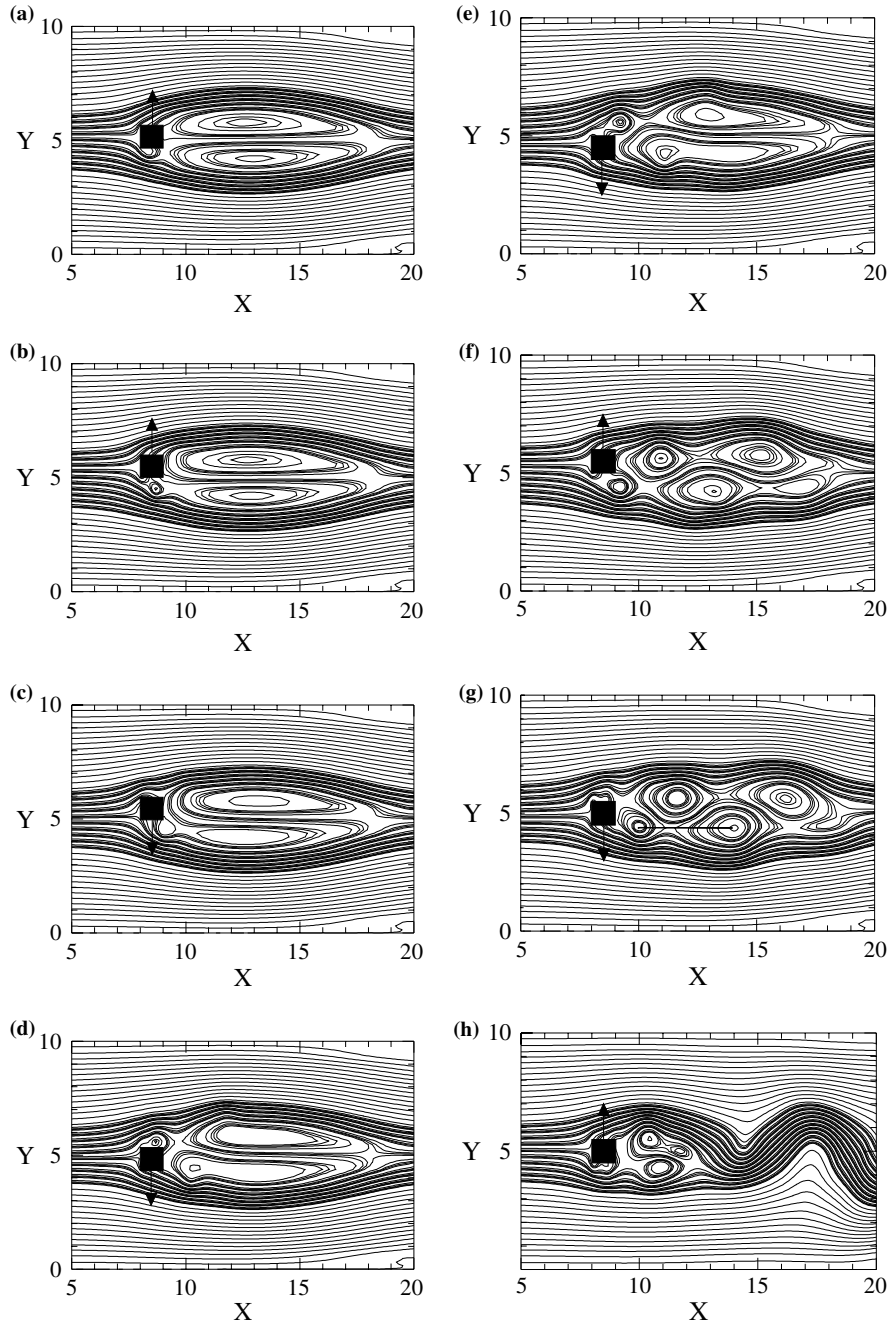

Fig. 4a–h The transient developments of the streamlines for case 1 **a** $\tau = 0.5$, **b** $\tau = 1.5$, **c** $\tau = 2.0$, **d** $\tau = 3.0$, **e** $\tau = 4.5$, **f** $\tau = 7.5$, **g** $\tau = 9.0$, **h** $\tau = 18.0$ **i** $\tau = 54.0$, **j** $\tau = 55.5$, **k** $\tau = 56.0$, **l** $\tau = 58.5$, **m** $\tau = 59.0$, **n** $\tau = 60.0$

Fig. 4 (continued)

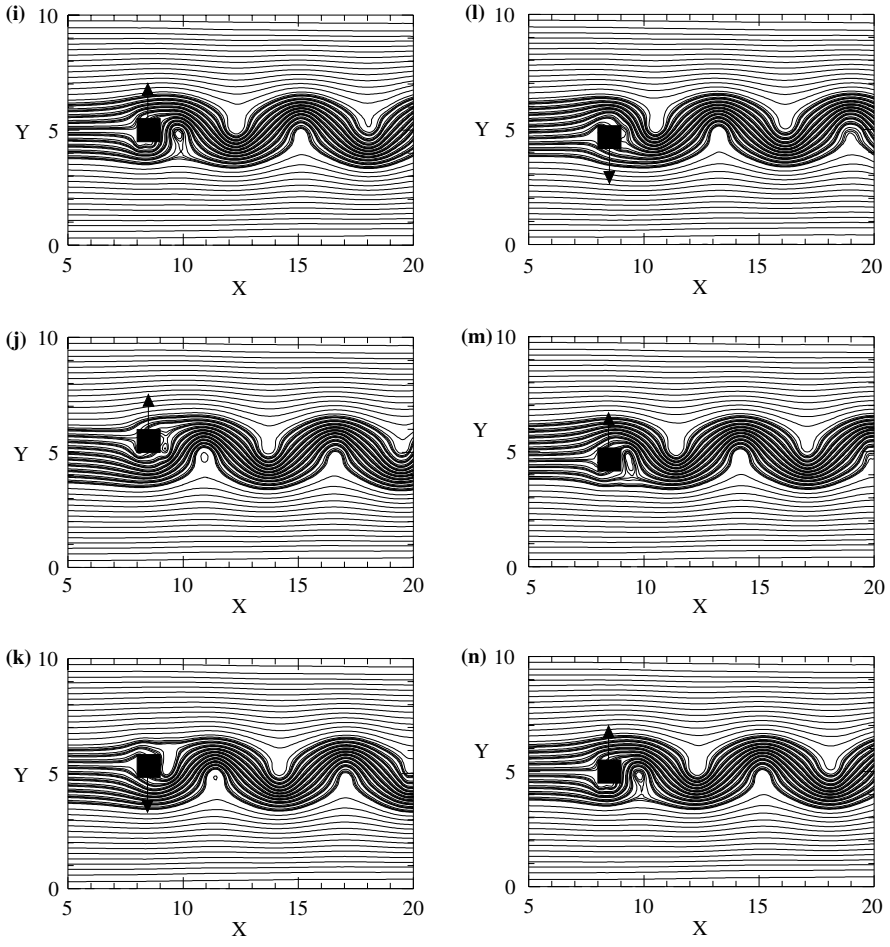

the results, the computational mesh with 74×54 elements is used for all the following cases. Besides, a backward scheme is adopted to deal with the time differential terms of the governing equations. The time step $\Delta\tau = 5.0 \times 10^{-3}$ is chosen for all cases in this study.

Furthermore, the residual of the continuity equation

$$\text{Re } sidual = \frac{\partial U}{\partial X} + \frac{\partial V}{\partial Y} \tag{12}$$

is used to check for each element at each time step and to ensure that the mass conservation law is satisfied. In the computing processes, the residual of the continuity equation for each element is smaller than 5.0×10^{-7} and the total residual of the continuity equation over the computational domain is smaller than 1.0×10^{-4}.

The attention of this study is focused on the variations of the flow structures in the wake because of the interaction between the oscillating rectangular cylinder and flow. The dimensionless stream function Ψ is defined as

$$U = \frac{\partial \Psi}{\partial Y} \text{ and } V = -\frac{\partial \Psi}{\partial X} \ . \tag{13}$$

For indicating the variations of the flow patterns in more details, except Fig. 3, which displays the overall computational domain, only the streamlines in the vicinity of the rectangular cylinder are presented. Besides, the arrow in the subsequent figures indicates the moving direction of the rectangular cylinder.

4.2 Effects of an oscillating rectangular cylinder on flow structures

Figure 3 shows the streamlines at the steady state ($\tau = 0$ and $V_m = 0$) under $\text{Re} = 500$ and $A = 1.0$ situation. The rectangular cylinder is stationary and the flow is steady. The flow around the rectangular cylinder separates from the leading edges of the rectangular cylinder and large recirculation zones are observed behind the rectangular cylinder.

Figure 4 shows the transient developments of the streamlines for case 1. Initially ($\tau = 0$), the rectangular cylinder is stationary at the center of the channel and the flow is steady. As the time $\tau > 0$, the rectangular cylinder is forced to oscillate with a velocity $V_m \cos(2\pi\Omega\tau)$, where $V_m = 0.333$ and $\Omega = 0.167$. At first, the rectangular cylinder moves upward, as shown in Fig. 4a. The fluid near the top surface of the rectangular cylinder is pressed by the top surface of the rectangular cylinder. Thus, the separation of flow from the leading edge of the top

surface of the rectangular cylinder is no longer to occur. In the meantime, the fluid near the bottom surface of the rectangular cylinder replenishes the vacant space induced by the movement of the rectangular cylinder because of the continuity of the flow. As a result, a new recirculation zone is observed around the bottom surface of the rectangular cylinder. Afterwards, the rectangular cylinder moves upward continuously until it reaches the maximum upper amplitude. The new recirculation zone around the bottom surface of the rectangular cylinder enlarges gradually and pushes the original large recirculation zones behind the rectangular cylinder, as shown in Fig. 4b.

The rectangular cylinder turns downward immediately as it reaches the maximum upper amplitude. As shown in Fig. 4c, d, the rectangular cylinder is on the way to move downward. The fluid near the top surface of the rectangular cylinder simultaneously replenishes the vacant space induced by the movement of the rectangular cylinder. Consequently, a new recirculation zone is formed around the top surface of the rectangular cylinder. Conversely, the fluid near the bottom surface of the rectangular cylinder is pressed by the bottom surface of the rectangular cylinder. As a result, the original recirculation zone around the bottom surface of the rectangular cylinder is pressed by the bottom surface of the rectangular cylinder and merged into the original large recirculation zones behind the rectangular cylinder. Afterwards, the rectangular cylinder moves downward continuously, and the new recirculation zone around the top surface of the rectangular cylinder enlarges gradually. As shown in Fig. 4e, the new recirculation zone around the top surface of the rectangular cylinder pushes the original large recirculation zones behind the rectangular cylinder away from the rectangular cylinder to become a shedding vortex.

As the rectangular cylinder reaches the maximum downward amplitude, the rectangular cylinder returns immediately. As shown in Fig. 4f, the rectangular cylinder is on the way to move upward. The recirculation zone around the top surface of the rectangular cylinder is pressed by the top surface of the rectangular cylinder, and then shed from the top surface of the rectangular cylinder. Furthermore, the recirculation zone around the bottom surface of the rectangular cylinder enlarges gradually and pushes the original large recirculation zones behind the rectangular cylinder to the downstream. Because of the oscillating motion of the rectangular cylinder and the vortices shedding, it is difficult for large recirculation zones behind the rectangular cylinder to maintain their original state. Thus, the original large recirculation zones behind the rectangular cylinder split into small vortices.

As the time increases, because the rectangular cylinder is in an oscillating motion, new recirculation zones are alternately formed and shed from the top and bottom surfaces of the rectangular cylinder, as shown in Figs. 4g, h. Because of the drastic swinging of the flow and the addition of vortex number in the region behind the rectangular cylinder, the vortices are contracted and entrained in the flow gradually, and the flow becomes a wavy flow. The interaction between the oscillating rectangular cylinder and shedding vortices dominates the state of the wake. The mechanisms of the vortex shedding and flow behavior are quit different from those of an oscillating circular cylinder, which the vortices shed from the rear region of the circular cylinder [27].

Figures 4i , n show the variations of the flow patterns during one cycle of the oscillation motion of the rectangular cylinder as the flow field reaches a periodic state. The flow pattern at the time $\tau = 54.0$ (Fig. 4i) is identical with that at the time $\tau = 60.0$ (Fig. 4n), which means that the variations of the flow field approach a periodic motion with time. Strouhal number, St, is equal to 0.167, which is identical to the oscillation frequency of the rectangular cylinder. In other words, the vortex shedding frequency is gradually changed to match the oscillation frequency of the rectangular cylinder and the flow field is in the lock-in state.

Figure 5 shows the time history of the velocity V at a position of $X = 10.0$ and Y at the center of the rear surface of the rectangular cylinder. After the time $\tau > 36.0$, the variations of the velocity V become a periodic function with time and Strouhal number is about 0.167, which is consistent with that mentioned above.

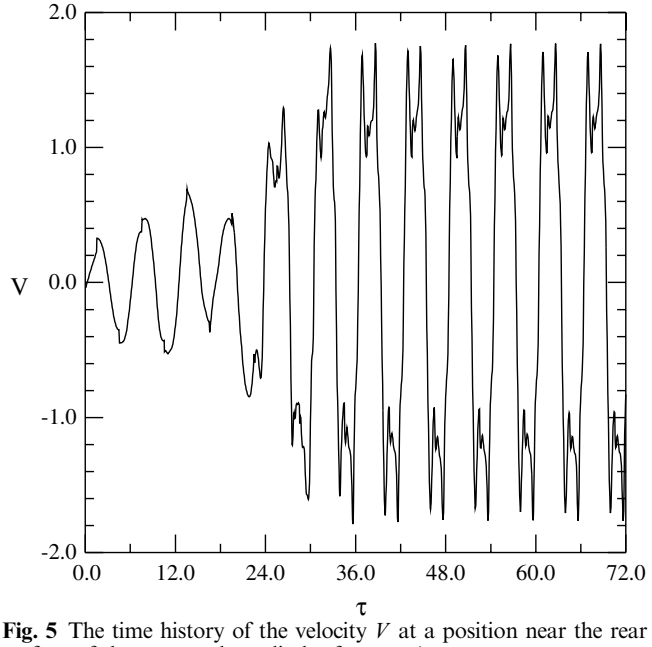

Fig. 5 The time history of the velocity V at a position near the rear surface of the rectangular cylinder for case 1

4.3 Effects of the maximum oscillating speed on flow structures

The transient developments of the streamlines for case 2 are shown in Fig. 6. In this case, the oscillating speed of

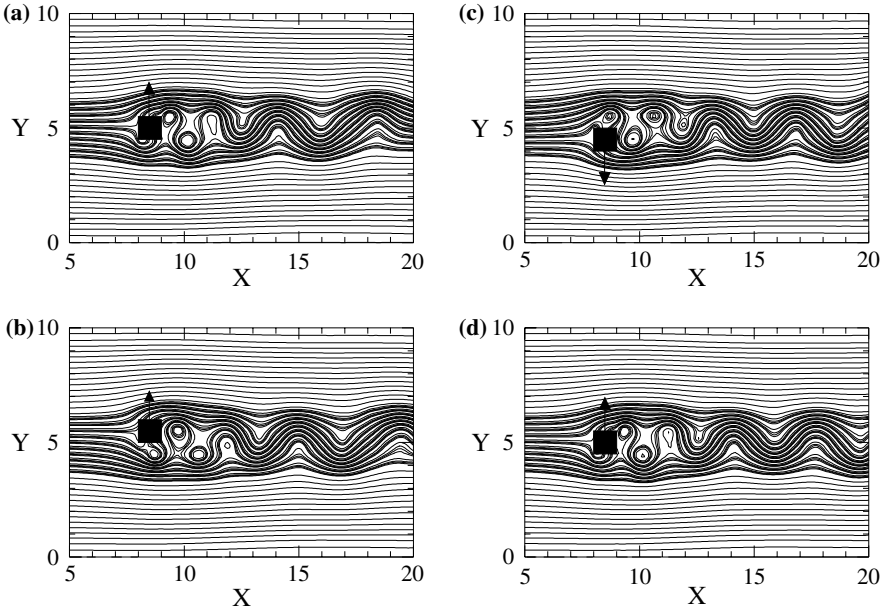

Fig. 6a–d The transient developments of the streamlines for case 2 **a** $\tau = 52.0$, **b** $\tau = 53.0$, **c** $\tau = 55.0$, **d** $\tau = 56.0$

the rectangular cylinder is faster than that of case 1. Basically, the variations of the flow field and the mechanisms of the vortex shedding from the rectangular cylinder are similar to case 1. The vortices shedding from the rectangular cylinder are entrained by the motion of the rectangular cylinder. Because the oscillating speed is larger in this case, the speed of vortices shedding from the rectangular cylinder is faster than that of case 1, and several small vortices are observed apparently behind the rectangular cylinder in the cyclic motion. These phenomena are somewhat different from those of case 1. The flow pattern at the time $\tau = 52.0$ (Fig. 6a) is identical to the one at the time $\tau = 56.0$ (Fig. 6d), and Strouhal number is equal to 0.25, which is identical to the oscillation frequency of the rectangular cylinder.

Figure 7 shows the time history of the velocity V at the position in the same as case 1. The results show that after the time $\tau > 48.0$ the variations of the velocity V become a periodic function with time. The time for the flow to reach a periodic state is slower than that of case 1. The reason is suggested as that the oscillating speed of the rectangular cylinder is faster than that of case 1, the variations of the flow field are more drastic in this case. The flow region affected by the oscillating rectangular cylinder in the traversing direction is smaller than that of case 1.

Figure 8 indicates the transient developments of the streamlines for case 3 as the flow had become a periodic motion with time. Because the oscillating speed of the rectangular cylinder is too large, recirculation zones around the top and bottom surfaces of the rectangular cylinder are immediately pressed by the rectangular cylinder and shed from the rectangular cylinder as these recirculation zones are formed. This behavior causes that the flow patterns behind the rectangular cylinder are virtually like no wake. The vortex shedding

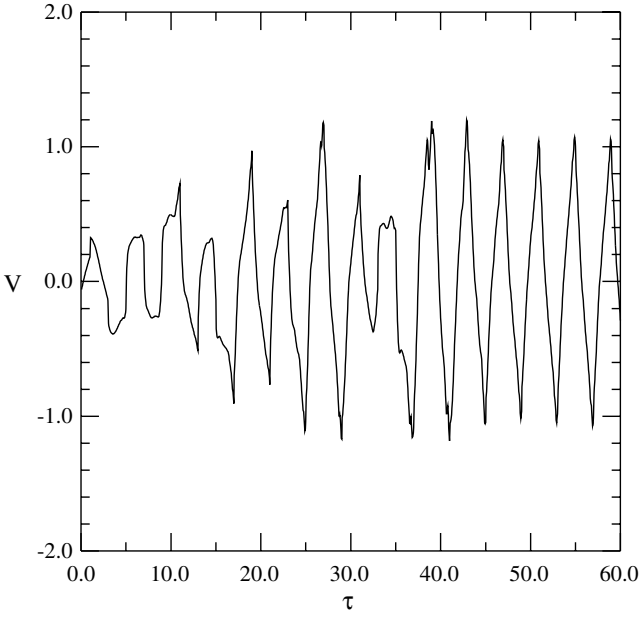

Fig. 7 The time history of the velocity V at a position near the rear surface of the rectangular cylinder for case 2

frequency is synchronized with the oscillation frequency of the rectangular cylinder. Strouhal number, which is equal to 0.5, is identical to the oscillation frequency of the rectangular cylinder.

4.4 Effects of the aspect ratio of the rectangular cylinder on flow structures

Figure 9 indicates the transient developments of the streamlines for case 4. The aspect ratio A is equal to 2.0

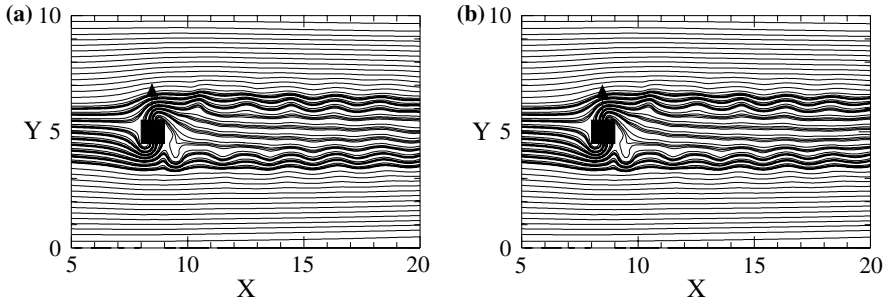

Fig. 8a, b The transient developments of the streamlines for case 3 **a** $\tau = 36.0$, **b** $\tau = 38.0$

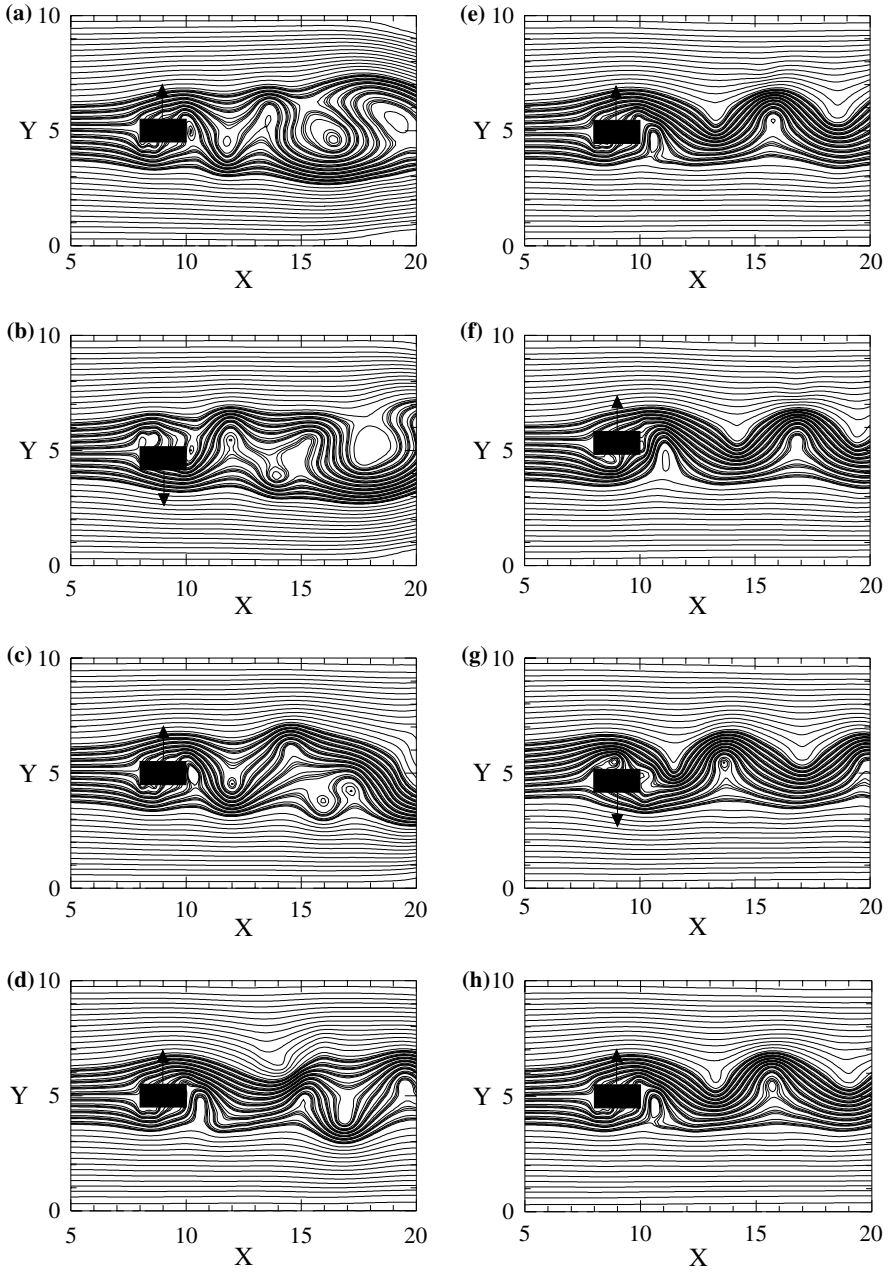

Fig. 9a–h The transient developments of the streamlines for case 4 **a** $\tau = 12.0$, **b** $\tau = 15.0$, **c** $\tau = 18.0$, **d** $\tau = 30.0$, **e** $\tau = 48.0$, **f** $\tau = 49.0$, **g** $\tau = 52.0$, **h** $\tau = 54.0$

in this case. In general, the variations of flow structures are similar to those of case 1. The increase in aspect ratio causes the effects of the oscillating rectangular cylinder on the flow to extend further downstream, and the flow region affected by the oscillating rectangular cylinder in the traversing direction is larger than that of case 1.

5 Conclusions

Flow characteristics of a rectangular cylinder oscillating in a channel flow are numerically investigated. Some conclusions are summarized as follows:

1. The interaction between the oscillating rectangular cylinder and vortices shedding from the rectangular cylinder dominates the state of the wake.
2. The vortices shedding from the rectangular cylinder are entrained by the motion of the rectangular cylinder. After an initial stage, the flow field becomes a periodic motion with time and the vortex shedding frequency is gradually changed to match the rectangular cylinder oscillation frequency. These phenomena are similar to the entrainment processes stated in Blackburn and Henderson [8] and the flow is in the lock-in state. This is quit different from an oscillating circular cylinder, which Strouhal number is equal to the oscillating frequency of the circular cylinder when only the oscillating frequency of the circular cylinder is near the nature frequency [28].
3. As the oscillating speed of the rectangular cylinder is too large, recirculation zones around the top and bottom surfaces of the rectangular cylinder are immediately pressed by the rectangular cylinder and shed from the rectangular cylinder as they are formed, and the flow patterns behind the rectangular cylinder are virtually like no wake.
4. The increase in the aspect ratio causes the effect of the oscillating rectangular cylinder on the flow to be more apparent.

Acknowledgements The support of this work by the National Science Council of Taiwan under contract NSC92-2212-E-252-001 and Nan Kai College under grant No. 92-26-C1201-21 is gratefully acknowledged.

References

Lin CL, Pepper DW, Lee SC (1976) Numerical methods for separated flow solutions around a circular cylinder. AIAA Journal 14:900–907

Benedict RP (1977) Flow-Induced Vibration, Van Nostrand Reinhold Company, New York, chapter 3

Hurlbut SE, Spaulding ML, White FM (1982) Numerical solution for laminar two dimensional flow about a cylinder oscillating in a uniform stream. J. Fluids Eng. 82:214–222

Lecointe Y, Piquet J (1989) Flow structure in the wake of an oscillating cylinder. J. Fluids Eng. 111:139–148

Hammache M, Gharib M (1991) An experimental study of the parallel and oblique vortex shedding from circular cylinders. J. Fluid Mech. 232:567–590

Inoue O, Yamazaki T, Bisaka T (1995) Numerical simulation of forced wakes around a cylinder. Int. J. Heat Fluid Flow 16:327–332

Zhang J, Dalton C (1997) Interaction of a steady approach flow and a circular cylinder undergoing forced oscillation. J. Fluids Eng. 119:808–813

Blackburn HM, Henderson RD (1999) A study of two-dimensional flow past an oscillating cylinder. J. Fluid Mech. 385:255–286

Davis RW, Moore EF (1982) A numerical study of vortex shedding from rectangles. J. Fluid Mech. 116:475–506

Okajima A (1982) Strouhal numbers of rectangular cylinders. J. Fluid Mech.123:379–398

Suzuki H, Inoue Y, Nishimura T, Fukutani K, Suzuki K (1993) Unsteady flow in a channel obstructed by a square rod: crisscross motion of vortex. Int. J. Heat Fluid Flow 14:2–9

Hwang RR, Yao CC (1997) A numerical study of vortex shedding from a square cylinder with ground effect. J. Fluids Eng. 119:512–518

Sohankar A, Norberg C, Davidson L (1998) Low-Reynolds -number flow around a square cylinder at incidence: study of blockage, onset of vortex shedding and outlet boundary condition. Int. J. Numer. Meth. Fluids 26:39–56

Chen JM, Liu CH (1999) Vortex shedding and surface pressures on a square cylinder at incidence to a uniform air stream. Int. J. Heat Fluid Flow 20:592–597

Zheng W, Dalton C (1999) Numerical prediction of force on rectangular cylinders in oscillating viscous flow. J. Fluids Structures 13:225–249

Hirt CW, Amsden AA, Cooks HK (1974) An arbitrary Lagrangian-Eulerian computing method for all flow speeds. J. Comput. Phys. 14:227–253

Hughes TJR, Liu WK, Zimmermann TK (1981) Lagrangian-Eulerian finite element formulation for incompressible viscous flows. Comput. Meth. Appl. Mech. Eng. 29:329–349

Donea J, Giuliani S, Halleux JP (1982) An arbitrary Lagrangian-Eulerian finite element method for transient dynamic fluid-structure interactions. Comput. Meth. Appl. Mech. Eng. 33:689–723

Ramaswamy B, Kawahara M (1987) Arbitrary Lagrangian-Eulerian finite element method for unsteady, convective, incompressible viscous free surface fluid flow. Int. J. Numer. Meth. Fluids 7:1053–1075

Ramaswamy B (1990) Numerical simulation of unsteady viscous free surface flow. J. Comput. Phys. 90:396–430

Reddy JN, Gartling DK (1994) The Finite Element Method in Heat Transfer and Fluid Dynamics, New York, CRC Press. Inc., chapter 4

Hueber KH, Thornton EA, Byrom TG (1995) The Finite Element Method for Engineers, third edition, John Wiley & Sons Inc., chapter 9

Irons BM (1970) A frontal solution program for finite element analysis. Int. J. Numer. Meth. Eng. 2:5–32

Taylor C, Hughes TG (1981) Finite Element Programming of the Navier-Stokes Equations, Pineridge Press Ltd., UK chapter 6

Fu WS, Yang SJ (2000) Numerical simulation of heat transfer induced by a body moving in the same direction as flowing fluids. Heat Mass Transfer 36:257–264

Yang SJ, Fu WS (2002) A numerical investigation of effects of a moving operator on airflow patterns in a cleanroom. Building Environment 37:705–712

Fu WS, Tong BH (2002) Numerical investigation of heat transfer from a heated oscillating cylinder in a cross flow. Int. J. Heat Mass Transfer 45:3033–3043

Cheng CH, Hong JL, Aung W (1997) Numerical prediction of lock-on state effect on convective heat transfer from a transversely oscillating circular cylinder. Int. J. Heat Mass Transfer 40:1825–1834